RESEARCH ARTICLE
Bull Biotechnol (2021) 2(2):27-31
https://doi.org/10.51539/biotech.1033344 Jurnal homepage: www.dergipark.org.tr/biotech

Bulletin of Biotechnology

The effect of the cross-linker ratio used in gellan gum biomaterial synthesis on biomineralization

Serbülent Türk[1,2,*], Burak Ünlü[1,2], Mahmut Özacar[2,3]

[*1]*Sakarya University, Biomedical, Magnetic and Semiconductor Materials Application and Research Center (BIMAS-RC), Sakarya University, Sakarya, Turkey*
[2]*Sakarya University, Biomaterials, Energy, Photocatalysis, Enzyme Technology, Nano & Advanced Materials, Additive Manufacturing, Environmental Applications and Sustainability Research & Development Group (BIOENAMS R & D Group), Sakarya University, Sakarya, Turkey*
[3] *Sakarya University, Faculty of Science & Arts, Department of Chemistry, Sakarya, Turkey*

*Corresponding author : serbulentturk@sakarya.edu.tr
Orcid No: https://orcid.org/ 0000-0003-4284-5397

Received : 08/12/2021
Accepted : 24/12/2021

Abstract: The first step in using polymeric materials for many applications is their crosslinking. The crosslinker used in crosslinking before application should be kept at an optimum ratio. The use of gellan gum (GG), a polymeric material, as an intra-body biomaterial is also among these application areas. In this study, the effect of the $CaCl_2$ ratio, used as GG crosslinker, was investigated on the biomineralization of GG hydrogel, which was successfully obtained from 2.5% (w/v) solutions. $GG_{0.5}$, $GG_{1.0}$, and $GG_{1.5}$ hydrogels obtained by crosslinking at 0.5, 1.0, and 1.5% were frozen at −20 °C for 12 h lyophilized at −50 °C at 15Pa for 2 days. FTIR, XRD, SEM, and EDS analyzes of cross-linked GG samples at different rates were performed before and after the biomineralization experiment, for which they were kept in a pre-prepared simulated body fluid medium for 7 days. As a result of the analysis, it was observed that the $GG_{1.0}$ sample, which has a homogeneous surface morphology, has higher P and Ca content and higher bioactivity than the $GG_{0.5}$ and $GG_{1.5}$ samples.

Keywords: Crosslinking; polymer; bioactivity.

1 Introduction

Hydrogels have been extensively studied in tissue engineering and continue to be investigated (Qian at al. 2022). Hydrogel systems consist of cross-linked polymers that can swell when placed in an aqueous medium and, thanks to this swelling feature, are also suitable for drug loading by filling the place where they are implanted. Hydrogels have an advantage over other biomaterials because they have porous structures similar to the extracellular matrix (Akther at al. 2020). In addition, due to their good biocompatibility, they can also be used as carrier materials for cells or bone growth to promote growth factors in bone tissue engineering. Hydrogels attract attention in the field of biomaterials because of their soft tissue adaptability to many soft tissues and their ability to reduce the inflammatory response of surrounding cells and tissues (Bendtsen and Wei, 2015; Tang et al. 2020). Gellan gum, a structure that can be classified as hydrogel, attracts increasing attention in the biomedical field thanks to its versatility and is recommended for tissue engineering applications (Costa et al. 2018; Omar et al. 2021).

Chemical crosslinking agents such as aldehydes, carbodiimides, epoxy and diisocyanates have been widely used in chemical preparation methods. However, most of these agents are toxic to humans. EDC and NHS (Hua et al. 2016), which are other generally used cross-linkers, can also pose a risk of cytotoxicity when used above certain concentrations. It can be used to adjust the elastic modulus of GG hydrogels obtained with crosslinking agents to that which is comparable to that of various human soft tissues such as cartilage. It is also known that the degradation rate is also affected by crosslinking (Choi et al. 2016; Maiti et al. 2021; Ye et al. 2018).

One of the important criteria in biomaterials developed for use in bone tissue engineering is bioactivity (Xue et al. 2018). Bioactivity experiments, in which the formation of bone

structure is examined before in vivo experiments, can be evaluated with in vitro tests (Kokubo and Takadama, 2006). For this, the method of immersion in simulated body fluid (SBF) is generally applied (Bano et al. 2021). Since polymeric hydrogels have certain limitations in the treatment of bone defects due to their poor bioactivity (Lin et al. 2021), these properties of polymeric hydrogels prepared as biomaterials need to be improved.

Although hydrogels have been widely studied for their physical and chemical stability, the bioactivities of these materials need to be improved. In this study, GG hydrogel samples with different crosslinker ratios were prepared. The obtained hydrogel samples were subjected to the bioactivity test. To the best of our knowledge, no study investigating the effect of cross-linking on bioactivity has been found so far.

2 Materials and Methods

Gellan gum (GG) and calcium chloride ($CaCl_2$), were purchased from Sigma Aldrich. Pure water obtained with Millipore Milli-Q was used throughout the study.

GG was dissolved in 2.5% (w/v) deionized water under constant stirring for 15 minutes at 85 °C. To prepare $GG_{0.5}$, $GG_{1.0}$ and $GG_{1.5}$ hydrogels, it is prepared by mixing with the ionic source of $CaCl_2$ at 85°C for 15 min, when used at a rate of 0.5, 1.0 and 1.5%, to be reduced at different rates. The prepared solutions were cooled to room temperature to obtain three-dimensional $GG_{0.5}$, $GG_{1.0}$ and $GG_{1.5}$ hydrogels. Before lyophilization, the hydrogels were frozen at −20 °C for 12 hours. Then, hydrogels were lyophilized at −50°C at 15Pa for 2 days (BIOBASE) after being kept in the pre-prepared SBF (Kokubo and Takadama, 2006) treatment for 7 days in sealed bottles.

Hydrogel samples were analyzed using FTIR (Spectrum Two Perkin-Elmer Co.) by scanning at 4 cm^{-1} resolution in the wavelength range of 4000 cm^{-1}-400 cm^{-1}. Morphological studies were observed using scanning electron microscopy (SEM, JEOL, JMS 6060). The hydrogels, which were previously lyophilized and cut into suitable pieces, were fixed on conductive carbon bands and then covered with a thin layer of gold to ensure conductivity (Polaron CS7620). The elemental distribution in the hydrogels obtained by energy dispersive X-ray spectroscopy (EDS) analysis was analyzed. For the phase characterization of the synthesized hydrogels, analysis was carried out between 5° and 90° using Cu Ka radiation (λ= 0.15406 nm) operating at 40 kV, 30 mA and X-ray diffractometry (XRD, D/Max 2200 LV).

3 Results and Discussion

SEM images of the hydrogel samples incubated for 7 d in SBF are shown in Fig. 1. It was observed that the apatite phase nucleated in the $GG_{1.5}$ sample was larger and less homogeneous compared to the other samples. In the $GG_{0.5}$ and $GG_{1.0}$ samples, a biomineralization process was observed in which homogeneity was preserved. Here, it is predicted that GG chains, which are more compact with the crosslinker effect, are less suitable for apatite nucleation compared to those with less crosslinker ratio. For this reason, it is thought that increasing the crosslinker ratio after a certain rate will affect the homogeneity of the natural bone to be formed in the body.

Elemental composition of $GG_{0.5}$, $GG_{1.0}$, and $OGG_{1.5}$ samples after incubation in SBF was analysed using EDS as shown in Table 1. The amounts of Ca and P elements resulting from CaP formation differ in hydrogel samples obtained by using different crosslinkers. Compared to the GG_1 hydrogel, a higher CaP accumulation was observed on the surfaces of the $GG_{1.0}$ and $GG_{1.5}$ hydrogel samples. Considering the SEM analyzes, due to the homogeneity on the $GG_{1.5}$ surface and the low formation on the $GG_{0.5}$ surface, the subsequent analyzes continued on $GG_{1.0}$, which was chosen as the optimum sample. $GG_{1.0}$ samples before and after immersion in SBF were named as "after GG" and "before GG" in the continuation of the study.

The phase composition was also confirmed by the FTIR. The FTIR spectra of before GG and after GG hydrogels are shown in Fig. 2. For the FTIR spectrum of before GG, the broad band at 3500−3000 cm^{-1} was contributed to stretching vibration of OH^- groups, the characteristic peak at 2925 cm^{-1} was attributed to the stretching vibration of $C–H_2$ groups, the characteristic peaks at 1611 and 1415 cm^{-1} were ascribed to the asymmetric and symmetric stretching vibration of carboxyl groups existed in the salt form, and 1032 cm^{-1} was attributed to the CO– stretching. It has been observed that the results are compatible with the literature (Mohd et al. 2020). Analysis of FTIR spectra of the sample incubated for 7 d in SBF confirms the presence of mineral deposits. Bands indicative for symmetric υ_1 and asymmetric stretching of the phosphate group in the regions 900–1150 cm^{-1}, and asymmetric bending of the PO_4^{3-} group in the region 500–650 cm^{-1}, were observed in after GG hydrogel sample. These peaks, which indicate biomineralization, were similarly observed in previous studies (Aneta et al. 2020; Huijie et al. 2020). This further demonstrated the analytical result of XRD.

Fig. 3 displays the X-ray diffraction pattern of after GG and before GG. GG showed a broad peak at approximately 2θ = 20°, indicated their amorphous nature with lower crystallinity. On comparing the XRD spectra of before GG and after GG, The diffractogram of before GG is typical of amorphous materials with no sharp peaks while diffractogram of after GG shows the sharp crystalline peaks (due to the nucleation of bioapatite) as shown by the presence of peaks at values of 26°, 32°, 33°, 34°, 40°, 46.5° and 49.5° 2θ, which correspond to the (002), (211), (300), (202), (310), (222) and (213) planes of bioapatite, respectively. Similar results for the same phase are also available in the literature (Hossein et al. 2022).

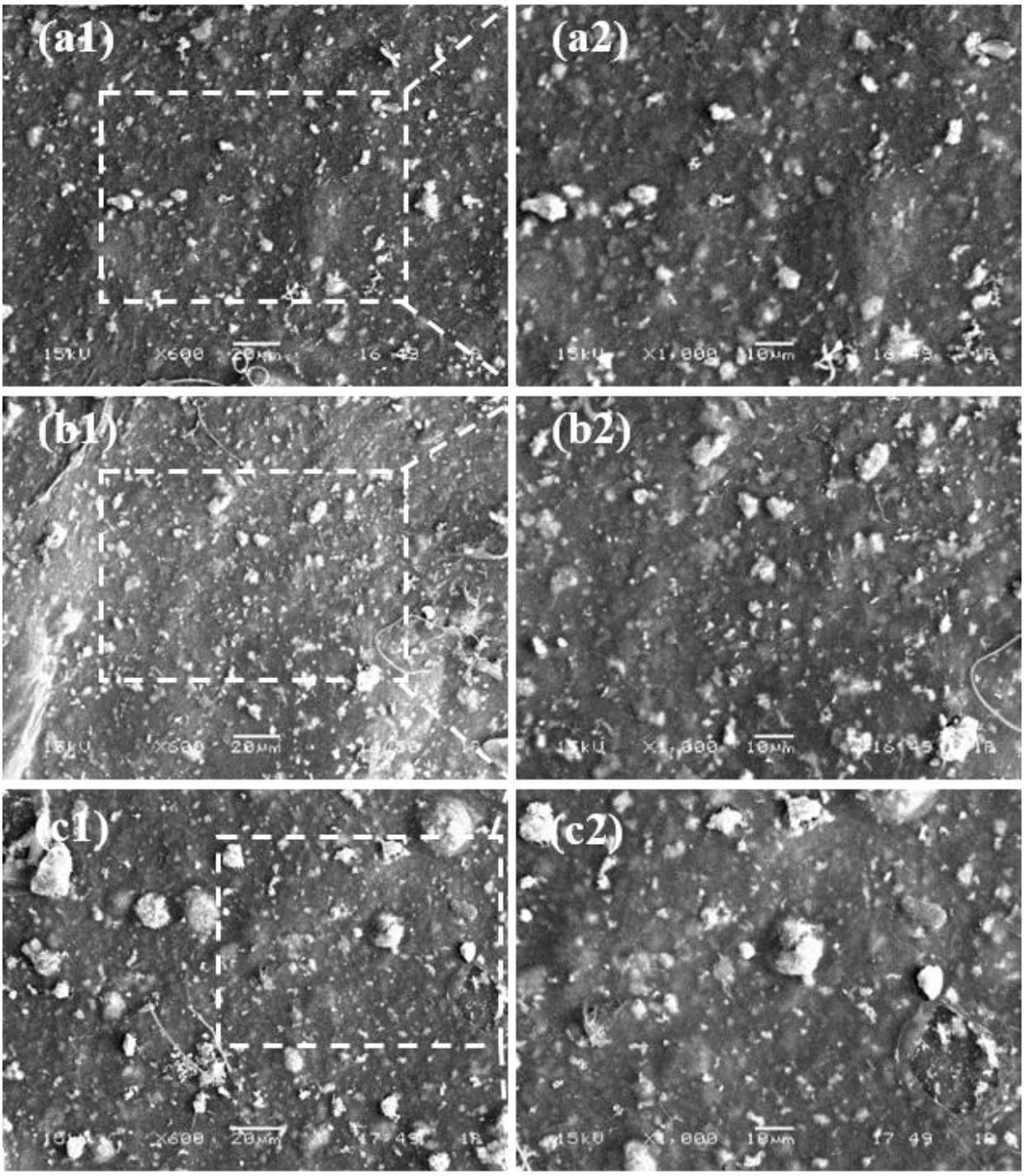

Figure 1. SEM images of (a1, a2) $GG_{0.5}$, (b1, b2) $GG_{1.0}$ and (c1, c2) $GG_{1.5}$ hydrogels.

Table 1. EDS determination of elemental C, O, P, and Ca atomic percentages in lyophilized hydrogels containing different cross linker ratio.

Hydrogel	C	O	P	Ca	Ca/P
	At. (%)				
$GG_{0.5}$	39.56	53.67	2.51	4.26	1.697
$GG_{1.0}$	39.07	51.79	3.41	5.73	1.680
$GG_{1.5}$	39.01	52.27	3.25	5.47	1.683

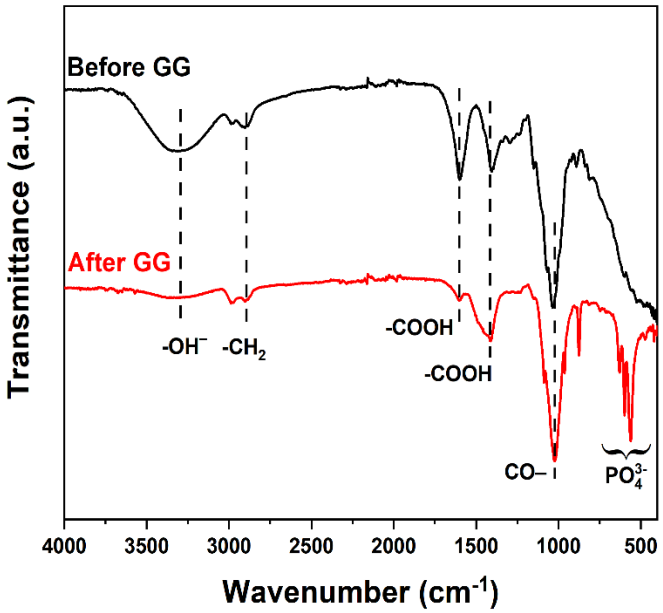

Figure 2. FTIR spectra of before GG and after GG hydrogel samples.

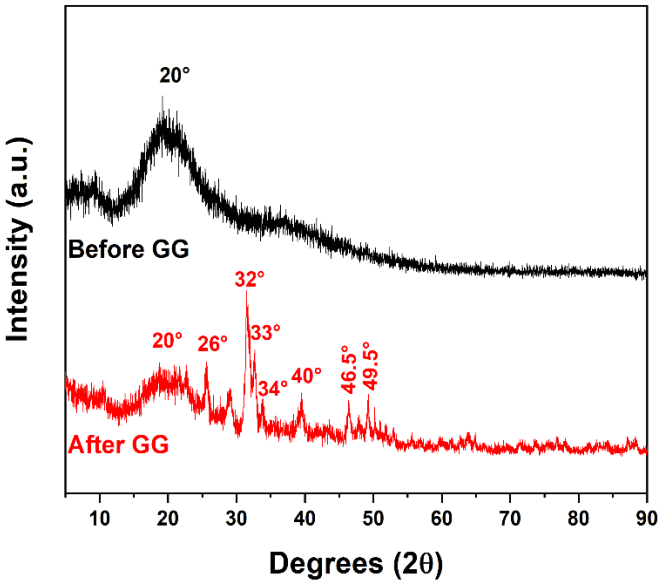

Figure 3. XRD pattern of the (a) before GG, and (b) after GG hydrogels.

4 Conclusion

In this study, hydrogel samples containing different ratios of crosslinker were prepared. In order to examine the bioactivation of the prepared hydrogels, they were kept in SBF for 7 days. Then, drying the hydrogels by lyophilization, the effects of crosslinker on activation were investigated. As a result of these examinations, it was observed that the crosslinker ratio of GG hydrogel affected the bioactivation. It has been found that the crosslinker ratios of GG based hydrogels, which can be used as biomaterials, should be determined before in-vivo studies, and this may contribute significantly to bioactivation and thus to bone formation.

Acknowledgments
This work was supported by the Scientific Research Projects Commission of Sakarya University (Project number: 2019-6-23-223).

Authors' contributions: The authors contributed equally to the article.

Conflict of interest disclosure: No potential conflict of interest was reported by the authors.

References

Akther F, Little P, Li Z, Nguyen N-T, Ta HT (2020) Hydrogels as artificial matrices for cell seeding in microfluidic devices. RSC Adv 10:43682-43703

Aneta P, Anna K, Marta W, Dorota L, Marta G, Andrzej B, Maria N (2019) Halloysite-alkaline phosphatase system—A potential bioactive component of scaffold for bone tissue engineering. Colloids and Surfaces B: Biointerfaces 173:1-8

Bano S, Rincon AR, Grant DM, Nommeots NA, Scotchford C, Ahmed I, Hussain T (2021) In-vitro cell interaction and apatite forming ability in simulated body fluid of ICIE16 and 13-93 bioactive glass coatings deposited by an emerging suspension high velocity oxy fuel (SHVOF) thermal spray. Surface and Coatings Technology 407:126764

Bendtsen ST, Wei M (2015) Synthesis and characterization of a novel injectable alginate-collagen-hydroxyapatite hydrogel for bone tissue regeneration. J Mater Chem B 3:3081–3090

Choi Y, Kim HJ, Min KS (2016) Effects of proanthocyanidin, a crosslinking agent, on physical and biological properties of collagen hydrogel scaffold. Restor Dent Endod 41:296

Costa L, Silva-correia J, Oliveira JM (2018) Gellan Gum-Based Hydrogels for Osteochondral Repair. In: S R J Oliveira J, Pina S, Reis R (ed), Osteochondral Tissue Engineering. Advances in Experimental Medicine and Biology, vol 1058. Springer, Cham

David O, Obada SA, Osseni HS, Kazeem AS, Ayodeji NO, David DA, Naresh DB, Stefan C, Abdulazeez YA, Opeoluwa OF, Adetunji RS, Laminu SK, Muhammad D, Johnson KA, Emmanuel TD (2021) Fabrication of novel kaolin-reinforced hydroxyapatite scaffolds with robust compressive strengths for bone regeneration. Applied Clay Science 215:0169-1317

Hossein K, Mohammad AP, Ali HM, Bahram P, Rouholah A (2022) Facile solution-based synthesis of impurity-free hydroxyapatite nanocrystals at ambient conditions. Journal of Materials Research and Technology 16:656-674

Hua J, Li Z, Xia W, Yang N, Gong J, Zhang J, Qiao C (2016) Preparation and properties of EDC/NHS mediated crosslinking poly (gamma-glutamic acid)/epsilon-polylysine hydrogels. Mater Sci Eng C 61:879–892

Huijie Z, Renchuan Y, Kun Y, Zhentan L, Qunmei F, Xiufang L, Dong W (2020) Silk as templates for hydroxyapatite biomineralization: A comparative study of Bombyx mori and Antheraea pernyi silkworm silks. International Journal of Biological Macromolecules 164:2842-2850

Kokubo T, Takadama H (2006) How useful is SBF in predicting in vivo bone bioactivity? Biomaterials 27:2907–2915

Lin H, Yin C, Mo A, Hong G (2021) Applications of Hydrogel with Special Physical Properties in Bone and Cartilage Regeneration. Materials 14: 235

Maiti S, Khillar PS, Mishra D, Nambiraj NA, Jaiswal AK (2021) Physical and self – crosslinking mechanism and characterization of chitosan-gelatin-oxidized guar gum hydrogel. Polym Test 97:107155

Mohd HR, Nur AI, Khairul AM (2020) Titanium dioxide nanotubes incorporated gellan gum bio-nanocomposite film for wound healing: Effect of TiO_2 nanotubes concentration, International Journal of Biological Macromolecules, Volume 153:1117-1135

Omar A, Lucilia PS, David C, Ricardo A, Subhas CK, Vitor MC, Rui LR (2021) Micropatterned gellan gum-based hydrogels tailored with laminin-derived peptides for skeletal muscle tissue engineering. Biomaterials 279:121217

Tang G, Tan Z, Zeng W, Wang X, Shi C, Liu Y, He H, Chen R, Ye X (2020) Recent Advances of Chitosan-Based Injectable Hydrogels for Bone and Dental Tissue Regeneration. Front Bioeng Biotechnol 8:1–15

Ye B, Zhang S, Li R, Li L, Lu L, Zhou C (2018) An in-situ formable and fi brils-reinforced polysaccharide composite hydrogel by self-crosslinking with dual healing ability. Compos Sci Technol 156:238–246

Qian Y, Jinrong P, Haitao X, Xuewen X, Zhiyong Q (2022) Polysaccharide hydrogels: Functionalization, construction and served as scaffold for tissue engineering. Carbohydrate Polymers 278:118952

Xue J, Feng C, Xia L, Zhai D, Ma B, Wang X, Fang B, Chang J, Wu C (2018) Assembly preparation of multilayered biomaterials with high mechanical strength and bone-forming bioactivity. Chem Mater 30:4646–4657